IOP Publishing Journal of Physics: Condensed Matter
J. Phys.: Condens. Matter **28** (2016) 266001 (7pp) doi:10.1088/0953-8984/28/26/266001

Complex incommensurate helicoidal magnetic ordering of $EuNiGe_3$

D H Ryan[1], J M Cadogan[2], Rasa Rejali[1] and C D Boyer[3]

[1] Physics Department and Centre for the Physics of Materials, McGill University, 3600 University Street, Montreal, Quebec, H3A 2T8, Canada
[2] School of Physical, Environmental and Mathematical Sciences, UNSW Canberra at the Australian Defence Force Academy, Canberra, ACT, BC 2610, Australia
[3] Canadian Neutron Beam Centre, Chalk River Laboratories, Ontario, Canada

E-mail: dhryan@physics.mcgill.ca

Received 16 March 2016, revised 20 April 2016
Accepted for publication 25 April 2016
Published 13 May 2016

Abstract

^{151}Eu Mössbauer spectroscopy and neutron powder diffraction are combined to show that the tetragonal ($I4mm$ #107) compound $EuNiGe_3$ orders magnetically below $T_N \sim 14$ K and adopts a complex incommensurate helicoidal magnetic structure at 3.6 K, with a propagation vector $\mathbf{k} = [0.255(1),\ 0.054(14),\ 0]$ and a Eu moment of 7.1(2) μ_B. On warming through 6 K an incommensurate sinusoidal modulation develops and dominates the magnetic order by 12 K.

Keywords: mossbauer spectroscopy, neutron diffraction, europium compounds, incommensurate order, magnetic structure

(Some figures may appear in colour only in the online journal)

1. Introduction

An initial study of magnetic ordering in tetragonal $EuNiGe_3$ suggested that it adopts a relatively simple collinear A-type antiferromagnetic (AF) structure below $T_N = 13.6$ K [1]. A later investigation using flux-grown single crystals combining bulk magnetic measurements with ^{151}Eu Mössbauer spectroscopy found that the ordering was far more complex [2]. In particular, the ^{151}Eu Mössbauer spectra suggested that the initial ordering observed at T_N (13.2 K in the single crystals [2]) was an incommensurate modulated AF structure which became commensurate below a second transition at 10.5 K.

The standard approach to determining magnetic structures is to use neutron diffraction, however europium's rather large absorption cross for thermal neutrons (4530 b) tends to discourage such measurements. Here we employ a large-area flat-plate technique to reduce the impact of the neutron absorption by natural europium [3]. This method has been applied successfully to study magnetic ordering in a variety of Eu-based [4, 5] and even Gd-based [6–8] compounds. We combine ^{151}Eu Mössbauer spectroscopy and neutron powder diffraction to show that the magnetic ordering in $EuNiGe_3$ remains incommensurate at least down to 3.6 K.

2. Experimental methods

The polycrystalline sample of $EuNiGe_3$ was synthesised from a stoichiometric mixture of the pure elements (Eu 99.9%, Ni 99.9% Ge 99.999%) using a solid state reaction of pressed powders following the method of Goetsch *et al* [1]. Small pieces of europium metal were pressed with a mixture of nickel and germanium powders to form a solid pellet. This was placed in a 2 cm^3 alumina crucible with a loosely fitting cap, sealed in a quartz tube under a partial pressure of pure helium and heated from 810 °C to 850 °C over a period of five hours. It was then reacted at 850 °C for three days. The resulting pellet, which had retained its original shape, was then powdered under hexane to avoid oxidation, re-pressed, wrapped in tantalum foil and annealed at 900 °C for seven days in a sealed quartz tube with a partial pressure of pure helium.

A second synthesis method was also found to work: the pure elements with 16% excess Eu were arc-melted. The resulting material was powdered under hexane, pressed into a pellet and then annealed at 900 °C for seven days as with the previous method. Both approaches yielded single-phased materials.

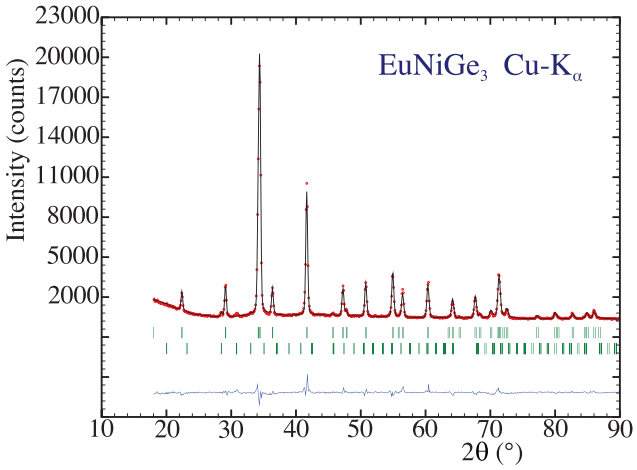

Figure 1. Room temperature Cu-K_α x-ray diffraction pattern of $EuNiGe_3$. The Bragg markers are (top): primary $EuNiGe_3$ phase, (bottom) Eu_2O_3 (∼1 wt.%).

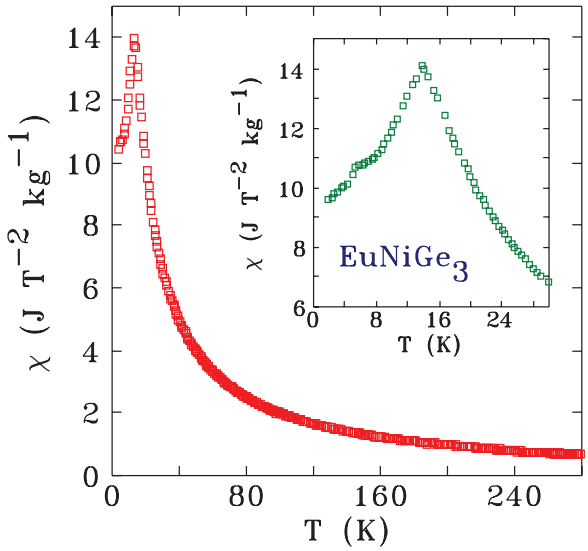

Figure 2. AC susceptibility data (1 kHz, 1 mT) taken on a quantum design physical properties measurement system (PPMS) for $EuNiGe_3$ showing the expected Curie–Weiss behaviour at high temperatures and the ordering cusp at 13.9(1) K. The inset shows the region below 27 K in more detail where the main cusp and the secondary feature at 5 K are more clearly visible.

Cu-K_α x-ray powder diffraction was used to confirm phase purity (figure 1) and confirm the expected structure (see table 1 for details). A small amount of Eu_2O_3 was detected (∼1 wt.%), probably introduced during grinding.

The ^{151}Eu Mössbauer spectroscopy measurements were carried out using a 4 GBq $^{151}SmF_3$ source, driven in constant acceleration mode. The drive motion was calibrated using a standard ^{57}CoRh/α-Fe foil. The 21.6 keV gamma rays were recorded using a thin NaI scintillation detector. The sample was cooled in a vibration-isolated closed-cycle helium refrigerator with the sample in a helium exchange gas. Temperature stability, as read by a calibrated cernox thermometer, was better than 0.01 K during each measurement. The methods used to fit the ^{151}Eu Mössbauer spectra are described later, where the data are presented.

Neutron powder diffraction experiments were carried out on the C2 800-wire powder diffractometer (DUALSPEC) at the NRU reactor, Chalk River Laboratories, Ontario, Canada, using neutron wavelengths (λ) of 1.3272(2) Å ('short', ∼1.33 Å) and 2.3676(3) Å ('long',∼2.37 Å). Diffraction patterns were obtained over the temperature range 3.6–20 K using a closed-cycle helium refrigerator. The sample mounting arrangement for this strongly-absorbing sample employs a large-area, flat-plate geometry [3] to reduce the impact of absorption by the europium.

Natural europium is a strong neutron absorber and its scattering length is dependent on the neutron energy, as tabulated by Lynn and Seeger [9], from which we derived the scattering length coefficient appropriate to our neutron wavelength: $\lambda \sim 1.33$ Å, $E = 46.3$ meV, $b_c = 6.9–0.9i$ fm; and $\lambda \sim 2.37$ Å, $E = 14.6$ meV, $b_c = 7.25–1.52i$ fm.

The *FullProf/WinPLOTR* suite of programs [10, 11] was used to fit the neutron diffraction patterns. Representational Analysis was carried out using the BASIREPS program [10, 11].

3. Results

Low-temperature ac susceptibility (1 kHz, 1 mT) revealed a conventional Curie–Weiss behaviour with a clear cusp centred at 13.9(1) K, consistent with the previous work on powder samples [1] but slightly higher than the 13.2 K reported for the single crystals [2]. The inset to figure 2 shows that we also observed the feature at ∼5 K reported previously [1]. The size of this feature was found to be somewhat sample dependent, which might lead one to attribute it to an unidentified impurity, however, it tended to be stronger in the cleaner (as determined by x-ray diffraction) samples, so we are inclined to suggest that it is intrinsic to $EuNiGe_3$.

3.1. ^{151}Eu Mössbauer spectroscopy

The room temperature ^{151}Eu Mössbauer spectrum of $EuNiGe_3$ consists of a single line with an isomer shift of −10.23(2) mm s^{-1}, confirming that the europium is fully divalent. On cooling to 5.6 K the line splits into a clearly magnetic pattern with a hyperfine field (B_{hf}) of 29.0(1) T consistent with values reported by Maurya *et al* [2], and in line with the expected contribution from ordered divalent europium in a single crystallographic site. However, on warming, the lines rapidly broaden towards the centre of the pattern as B_{hf} decreases and it is clear that the behaviour is more complex. Fitting the spectra shown in figure 3 with a single Eu^{2+} site and a linewidth constrained to that observed for the 5.6 K pattern yields very poor fits above 7 K (solid green lines in figure 3).

We turn therefore to a model that derives a distribution of hyperfine fields from an (assumed) incommensurate sinusoidally modulated magnetic structure based on one that was used previously by Maurya *et al* [2] to fit their ^{151}Eu Mössbauer spectra of $EuNiGe_3$. Variations of this model have also been used to fit spectra of EuPdSb [12] and Eu_4PdMg [13]. If we assume that the AF moment modulation along the direction of

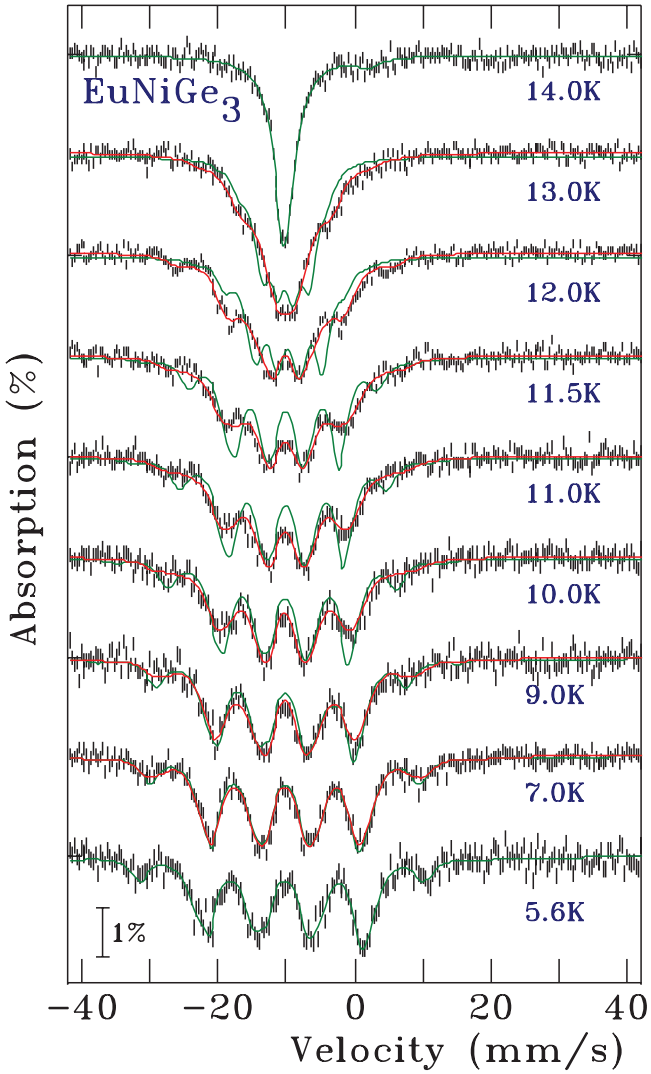

Figure 3. ^{151}Eu Mössbauer spectra of $EuNiGe_3$ measured between 14 K and 5.6 K showing the development of magnetic order. The feature near 0 mm s^{-1} evident in the 14 K spectrum is due to a 4(1)% Eu^{3+} impurity, identified as Eu_2O_3 in both the x-ray data (figure 1) and the neutron diffraction patterns (*vide infra*). Two fits are shown. The green solid lines show fits using a simple one-site, fixed linewidth magnetic model, while the solid red lines show a fit assuming an incommensurate sinusoidally modulated magnetic structure (see text for details).

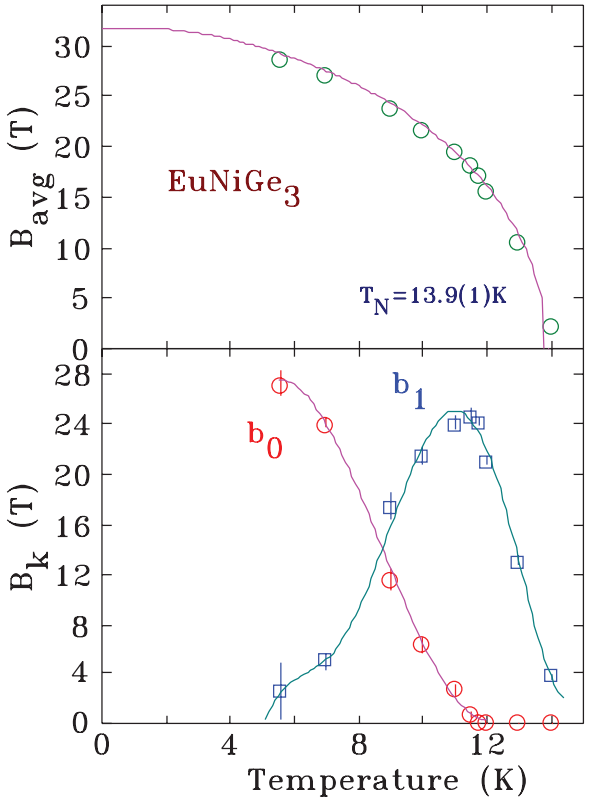

Figure 4. Results derived from the sinusoidally modulated fits to the ^{151}Eu Mössbauer spectra shown in figure 3. The top panel shows the average hyperfine field fitted with a $J = \frac{7}{2}$ Brillouin function to yield a transition temperature of 13.9(1) K, fully consistent with the value derived from ac susceptibility in figure 2. The lower panel shows the temperature dependence of the first two Fourier components in equation (1). At 5.6 K the constant term (b_0) dominates and the Eu appears to be in a uniform environment. However the b_1 term grows rapidly on warming as a sinusoidally modulated structure develops.

the propagation vector **k** can be written in terms of its Fourier components, and further assume that the observed hyperfine field is a linear function of the Eu moment at any given site, then the variation of $B_{\rm hf}$ with distance x along the propagation vector **k** can be written as:

$$B_{\rm hf}(k\,x) = b_0 + \sum_{l=0}^{n} b_{2l+1} \sin(2l+1)kx \qquad (1)$$

where the b_n are the odd Fourier coefficients of the field modulation. As $+B_{\rm hf}$ and $-B_{\rm hf}$ are indistinguishable, kx only needs to run over half the modulation period, and in this case, a square-wave modulated structure can be modelled either as a sum over a very large number of Fourier coefficients, or by simply using the b_0 term with all of the other b_n set to zero. We found the fits to be far more stable with the b_0 term included rather than using a large set of b_n, however the two approaches are effectively equivalent.

The modulated fitting model adds only one or two more parameters to the fit (b_1 and b_3, in addition to b_0) yet the solid red lines in figure 3 clearly fit the measured spectra far better than the simple 1-site model (equivalent to using only the b_0 term). The average hyperfine field (shown in the top panel of figure 4 fits to a $J = \frac{7}{2}$ Brillouin function to yield a transition temperature of 13.9(1) K, fully consistent with the value derived from ac susceptibility in figure 2. The lower panel of figure 4 shows the temperature dependence of the first two Fourier coefficients and the evolution from a constant Eu environment, where b_1 is zero, through an increasingly modulated environment as the temperature is increased until by 12 K the b_0 term vanishes and only the simple sinusoidal b_1 term and the first odd harmonic (b_3, not shown) remain. We see no evidence for an abrupt transition and it appears that the magnetic structure evolves continuously with increasing temperature until $T_{\rm N}$ is reached. It is possible that the 5 K feature in the ac susceptibility in figure 2 marks the onset (on warming) of a changeover from constant to modulated ordering, however our data do not extend far enough through this region to be

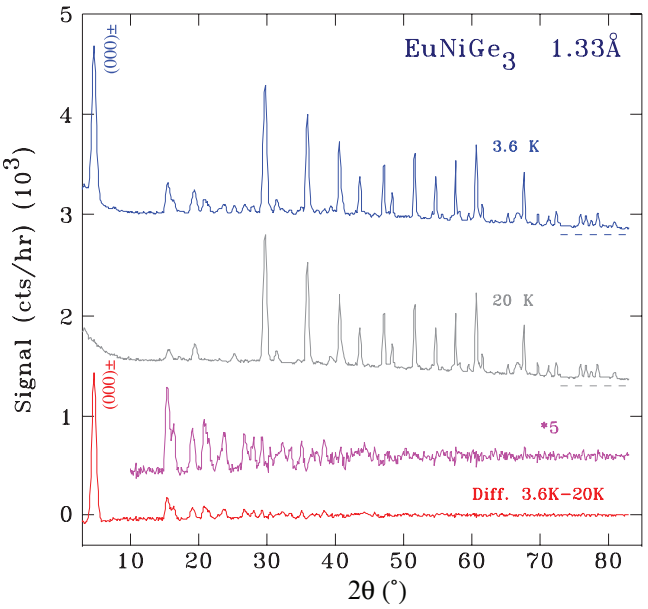

Figure 5. Neutron powder diffraction patterns for $EuNiGe_3$ measured with a wavelength of ∼1.33 Å and taken at (top) 3.6 K and (middle) 20 K showing the development of magnetic scattering from the ordered europium moments (most notably at $2\theta \sim 4.6°$—indexed as the (0 0 0) ± k peak). The bottom pattern shows the difference between the 20 K and 3.6 K data with a section multiplied by a factor of five to make the many weaker magnetic peaks more apparent.

sure. Looking at the behaviour on cooling it is clear that the initial order established near 14 K is purely modulated and the constant term (b_0) only appears below 12 K. Further cooling then leads to a gradual evolution towards a single environment for the Eu moments. However, significant modulation persists through 7 K, an observation that is inconsistent with an earlier suggestion based on more limited ^{151}Eu Mössbauer data that there is an incommensurate to commensurate transition at 10.5 K [2].

We turn now to neutron diffraction in order to determine the precise nature of this incommensurate modulated AF magnetic ordering.

3.2. Neutron diffraction

Comparison of neutron powder diffraction patterns taken at 20 K and 3.6 K using a wavelength of ∼1.33 Å presented in figure 5 clearly shows that the ordering of the europium moments in $EuNiGe_3$ is incommensurate. The magnetic pattern is dominated by a low-angle peak (at $2\theta \sim 4.6°$) that is stronger than any of the nuclear peaks and whose d-spacing (∼16.6 Å) does not correspond to an integral multiple of any of the crystal axes. There are many more weak magnetic peaks in the range $14° \leqslant 2\theta \leqslant 30°$ that also cannot be indexed simply to the crystallographic cell.

Fitting the intensity of the $(0\ 0\ 0)^{\pm}$ peak (using data taken with $\lambda \sim 2.37$ Å which moves it out to a higher 2θ where it is better isolated from the direct beam) to a squared $J = \frac{7}{2}$ Brillouin function yields a transition temperature of 14.5(1) K (see bottom panel of figure 6), slightly higher than that derived

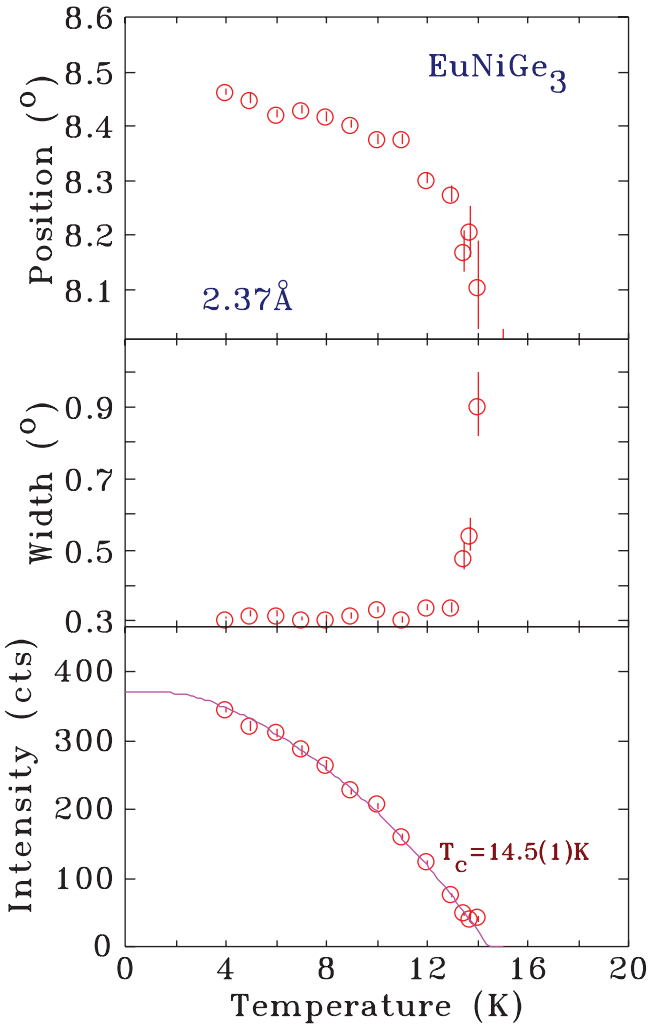

Figure 6. Temperature dependence of (top) position (middle) width and (bottom) intensity of the $(0\ 0\ 0)^{\pm}$ magnetic peak from the europium ordering. Note the significant changes in width and position as T_N is approached from below. The solid line through the intensity data is a fit to a $J = \frac{7}{2}$ squared Brillouin function giving T_N =14.5(1) K.

from χ_{ac} or Mössbauer spectroscopy. The top panel of figure 6 shows that the $(0\ 0\ 0)^{\pm}$ peak gradually moves to lower angles (i.e. the modulation period increases) up to about 12 K (where the constant term, b_0, reaches zero in the Mössbauer fits in figure 4). Above 12 K, the movement to lower angles accelerates and the peak broadens rapidly, reaching about three times our resolution limit before it is lost to the background (middle panel of figure 6). Contrary to earlier claims [2], it is clear from the behaviour shown on the top panel of figure 6 that the magnetic ordering in $EuNiGe_3$ is *never* commensurate. The position of the $(0\ 0\ 0)^{\pm}$ peak evolves continuously on cooling but never locks in to a commensurate location.

In table 2 we give the refined atomic positions and lattice parameters of $EuNiGe_3$, deduced from the co-refinement of the 20 K neutron powder diffraction patterns, obtained with $\lambda \sim 1.33$ Å and 2.37 Å. At 20 K, the scattering is purely nuclear. The top panel of figure 7 shows the full refinement of the neutron diffraction pattern of $EuNiGe_3$ obtained at

Table 1. Crystallographic data for $EuNiGe_3$ obtained by refinement of the 295 K Cu-K_α x-ray powder diffraction pattern.

Atom	Site	x	y	z
Eu	2a	0	0	0
Ni	2a	0	0	0.6520(4)
Ge	2a	0	0	0.4182(7)
Ge	4b	0	1/2	0.2569(7)

$a = 4.3296(3)$ Å $c = 9.8762(8)$ Å
R(Bragg) = 6.5
R(F) = 5.8

Note: It adopts the tetragonal $BaNiSn_3$-type structure (space group *I4mm* #107). N.B. The z atomic position parameter is not fixed by symmetry for *any* of the sites in the *I4mm* space group, and therefore any convenient point may be chosen for one atom (this amounts to selecting the origin for the cell). We set it to zero for the Eu atom in the 2*a* site and the z-parameters for the remaining atoms are then determined relative to this choice of origin.

Table 2. Crystallographic data for $EuNiGe_3$ obtained by co-refinement of the 20 K neutron powder diffraction patterns.

Atom	Site	x	y	z
Eu	2a	0	0	0
Ni	2a	0	0	0.653(2)
Ge	2a	0	0	0.419(2)
Ge	4b	0	1/2	0.257(1)

$a = 4.326(2)$ Å $c = 9.867(3)$ Å
R(Bragg) = 4.4
R(F) = 3.0
R(struct.) = 3.90

Note: The space group is tetragonal *I4mm* (#107). See caption for table 1 for a discussion of the origin choice.

20 K with $\lambda \sim 1.33$ Å. About 4 wt.% of Eu_2O_3 was found to be present (as noted in the analysis of the Mössbauer data above) and this impurity was included in all of the fits presented here.

As noted above, the many new magnetic diffraction peaks that appear at 3.6 K are incommensurate with the underlying tetragonal lattice. To identify the propagation vector **k** describing this magnetic structure we used the program *k-search*, part of the WinPlotr package [11]. The best fit to the magnetic peak positions was with **k** ∼[0.26, 0.06, 0].

Representational Analysis using the BASIREPS program [10, 11] showed that the magnetic representation for the Eu(2a) site is completely general:

$$\Gamma^{2a}_{\text{Mag}} = 3\Gamma^{(1)}_1 \qquad (2)$$

with the basis vector [u, v, w]. Magnetic contributions from the nickel and germanium sites were not considered.

Refinements of the 3.6 K diffraction patterns showed two possible magnetic structures, either a sinusoidal modulation or a helicoidal arrangement of the Eu moments. We also tried a square-wave modulation and a quadrupled commensurate structure (given that **k** is close to [1/4, 0, 0] but both of these options gave significantly worse refinements to the experimental data and were not considered further. The refined lattice parameters are $a = 4.324(2)$ Å and $c = 9.864(3)$ Å with a propagation vector $\mathbf{k} = [0.255(1), 0.054(14), 0]$.

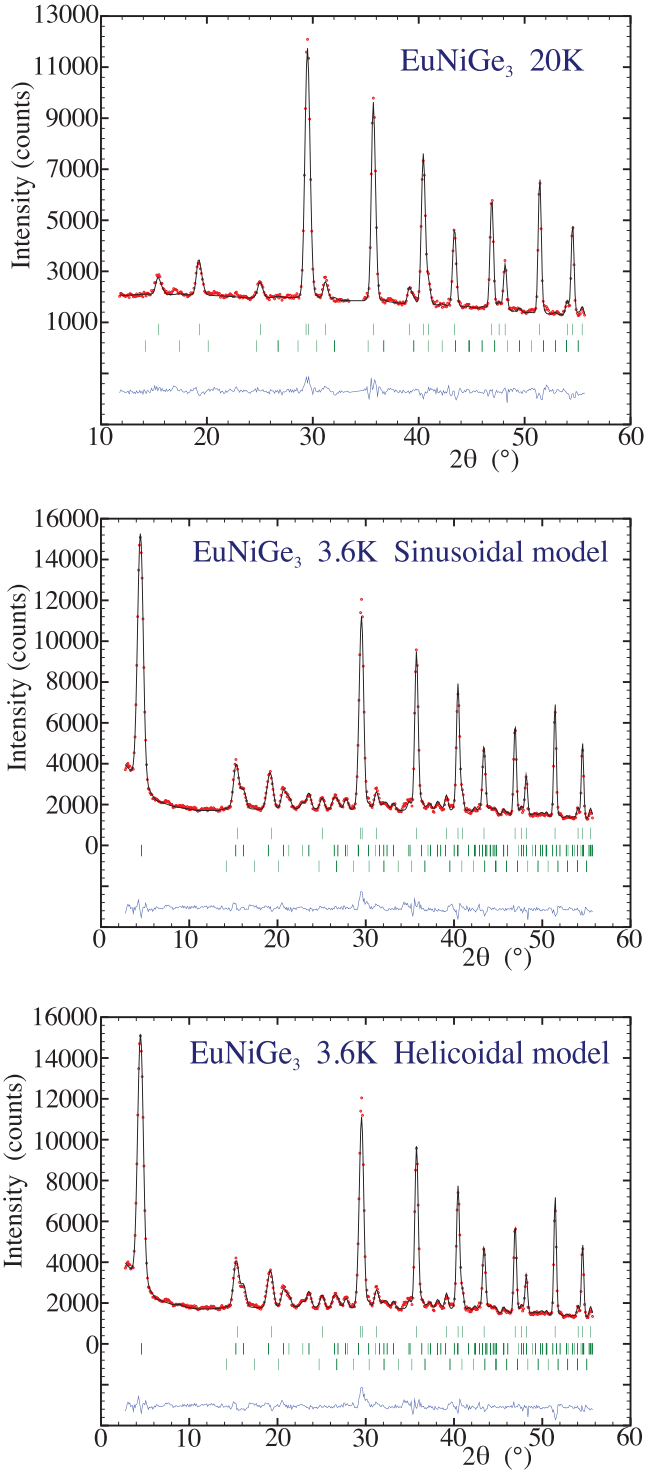

Figure 7. Neutron powder diffraction patterns of $EuNiGe_3$ measured with $\lambda \sim 1.33$ Å. The top panel shows the nuclear-only pattern recorded at 20 K, with Bragg markers for $EuNiGe_3$ (top) and 4 wt.% Eu_2O_3 impurity. The centre and bottom panels show the data recorded at 3.6 K. The patterns were fitted using a sinusoidally modulated magnetic structure (centre) and a helicoidal magnetic structure (bottom). In each case the Bragg markers are (top to bottom) $EuNiGe_3$ (nuclear) $EuNiGe_3$ (magnetic) and 4 wt.% Eu_2O_3 impurity. The description of the two magnetic models is given in the text.

If we assume a sinusoidally modulated magnetic structure, the refinement gives Fourier components of [3.72(6), 4.77(5), 7.88(7)] leading to a Fourier amplitude of 9.93 μ_B

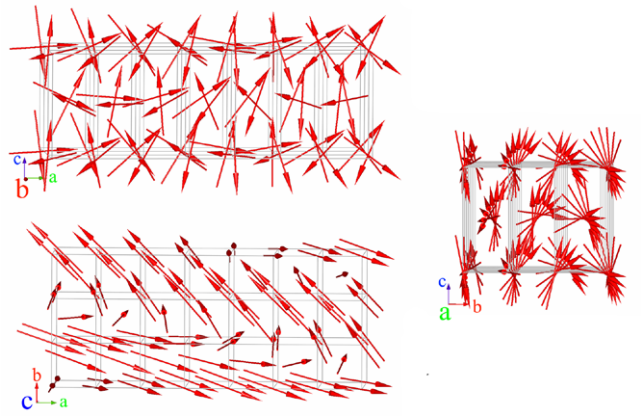

Figure 8. Calculated spin structure for $EuNiGe_3$ at 3.6 K derived from the helicoidal model described in the text. Several unit cells have been stacked in order to better visualise the complex incommensurate helicoidal structure and we show views taken looking (approximately) down the *a*, *b* and *c* axes.

and thus a moment amplitude of 7.0(3) μ_B. The fit, shown in the central panel of figure 7, gave goodness-of-fit parameters of: $R(\text{Bragg}) = 12.4$, $R(\text{F}) = 7.7$, $R(\text{Mag}) = 6.6$, $R_p = 17.5$, $R_{wp} = 14.8$, $R_{exp} = 7.1$ and $\chi^2 = 5.3$.

Alternatively, if we assume a helicoidal structure (fit shown in the lowest panel of figure 7) then we obtain an Eu moment of 7.1(2) μ_B. The polar angles describing the conical axis are: $\theta = 90°$ and $\phi = 32(2)°$. The refinement returned goodness-of-fit parameters of: $R(\text{Bragg}) = 14.1$, $R(\text{F}) = 10.1, R(\text{Mag}) = 7.8, R_p = 17.2, R_{wp} = 14.2, R_{exp} = 7.1$ and $\chi^2 = 4.1$.

In both cases the refinements used the $I\bar{1}$ space group, however for our initial analysis of the helicoidal structure we employed the $P\bar{1}$ group so that we could explore the possibility of there being a magnetic phase difference between the two Eu moments related by the '*I*' translation. Our $P\bar{1}$ refinements showed that any such phase difference was zero, within error, confirming that the $I\bar{1}$ group is appropriate.

It is not possible to choose between the two models using either goodness-of-fit criteria (χ^2 is slightly better for the helicoidal model, but the R-factors are slightly better for the sinusoidal model) or visual inspection of the fits shown in figure 7, so it is clear that neutron diffraction data alone cannot provide an unequivocal determination of the magnetic structure at 3.6 K. However, the two models predict quite different local magnetic environments for the Eu ions, and hence different ^{151}Eu Mössbauer spectra. For the helicoidal model, only the *direction* of the Eu moments changes as we pass through the lattice; their *magnitude* is constant. Thus we would expect a single-valued B_{hf} spectrum, perhaps with some line broadening due to the varying projection of B_{hf} onto V_{zz}. By contrast, the sinusoidally modulated model predicts a strong variation in the *magnitudes* of the Eu moments and hence in B_{hf}. It is clear from the spectra in figure 3 and the analysis shown in figure 4 that by 5.6 K the ^{151}Eu Mössbauer spectrum of $EuNiGe_3$ consists of a single-field magnetic pattern. We therefore conclude that the helicoidal structure is the one adopted by $EuNiGe_3$ at 3.6 K. Such structures are not unknown in the $RTGe_3$ compound family and a complex co-existing commensurate–incommensurate helicoidal magnetic structure has been reported in $CeNiGe_3$ [14]. Several views of the complex spin structure deduced for $EuNiGe_3$ at 3.6 K are shown in figure 8.

On warming through 6 K however, the magnetic structure changes and the ^{151}Eu Mössbauer data shown in figures 3 and 4 reveal that a sinusoidal modulation develops and that this modulated form dominates by 12 K. Analysis of diffraction patterns taken at 12 K suggests that the sinusoidal model gives a slightly fit than the helicoidal model, but the difference is not large. Given the small differences in fit quality both at 3.6 K and 12 K it is apparent that neutron powder diffraction diffraction *alone* cannot distinguish between the two models, however the complementary information provided by ^{151}Eu Mössbauer spectroscopy permits an unambiguous determination.

We find that $EuNiGe_3$ adopts a complex incommensurate helicoidal magnetic structure at 3.6 K, and that an incommensurate sinuoidal modulation develops on warming through 6 K. The modulated form dominates by 12 K and the final transition at 14 K to the paramagnetic state does not appear to be a conventional second order phase transition. Rather, the event is marked by a collapse of the long-range ordered state as the modulation period grows rapidly and the correlation length of the magnetic order decreases.

A recent single crystal study of $EuNiGe_3$ using short-wavelength (0.9 Å) neutrons reported a helicoidal structure with $\mathbf{k} = [\frac{1}{4}, 0.05, 0]$ at 1.6 K [15] in broad agreement with our results. However the improved resolution and access to the low-angle $(0\,0\,0)^{\pm}$ peak afforded by the longer neutron wavelengths allow us to show that the structure is incommensurate along both the *a*- and *b*- axes.

4. Conclusions

A combination of ^{151}Eu Mössbauer spectroscopy and neutron powder diffraction shows that $EuNiGe_3$ adopts a complex incommensurate helicoidal magnetic structure at 3.6 K, with a propagation vector $\mathbf{k} = [0.255(1), 0.054(14), 0]$ and a Eu moment of 7.1(2) μ_B. On warming through 6 K a sinusoidal modulation develops and dominates the magnetic order by 12 K. While the ^{151}Eu Mössbauer data leave no doubt that the modulation develops, the strong similarity between the diffraction patterns produced by the helicoidal and sinusoidal models precludes neutron powder diffraction from following the evolution of the magnetic structure on warming in any detail, but it is clear that the order remains incommensurate at all temperatures below $T_N \sim 14$ K.

Acknowledgments

Financial support for this work was provided by the Natural Sciences and Engineering Research Council of Canada, the Fonds Québécois de la Recherche sur la Nature et les Technologies and The University of New South Wales.

DHR acknowledges the award of a Rector-funded Visiting Fellowship by UNSW Canberra.

References

[1] Goetsch R J, Anand V K and Johnston D C 2013 *Phys. Rev.* B **87** 064406
[2] Maurya A, Bonville P, Thamizhavel A and Dhar S K 2014 *J. Phys.: Condens. Matter* **26** 216001
[3] Ryan D H and Cranswick L M D 2008 *J. Appl. Cryst.* **41** 198
[4] Ryan D H, Cadogan J M, Xu S, Xu Z and Cao G 2011 *Phys. Rev.* B **83** 132403
[5] Rowan-Weetaluktuk W N, Lemoine P, Cadogan J M and Ryan D H 2014 *J. Appl. Phys.* **115** 17E101
[6] Ryan D H, Cadogan J M, Cranswick L M D, Gschneidner K A, Pecharsky V K and Mudryk Y 2010 *Phys. Rev.* B **82** 224405
[7] Lee-Hone N R, Ryan D H, Isnard O, Diop L V and Cadogan J M 2013 *J. Appl. Phys.* **113** 17E119
[8] Ryan D H, Mas N, Susilo R A, Cadogan J M and Flacau R 2015 *J. Phys.: Condens. Matter* **27** 146005
[9] Lynn J E and Seeger P A 1990 *At. Data Nucl. Data Tables* **44** 191
[10] Rodríguez-Carvajal J 1993 *Physica* B **192** 55
[11] Roisnel T and Rodríguez-Carvajal J 2001 *Mater. Sci. Forum.* **378–81** 118
[12] Bonville P, Hodges J A, Shirakawa M, Kasaya M and Schmitt D 2001 *Eur. Phys. J.* B **21** 349
[13] Ryan D H, Legros A, Niehaus O, Pöttgen R, Cadogan J M and Flacau R 2015 *J. Appl. Phys.* **117** 17D108
[14] Durivault L, Bourée F, Chevalier B, André G, Weill F, Etourneau J, Martinez-Samper P, Rodrigo J G, Suderow H and Vieira S 2003 *J. Phys.: Condens. Matter* **15** 77
[15] Fabréges X, Gukasov A, Bonville P, Maurya A, Thamizhavel A and Dahr S K 2016 *Phys. Rev.* B (submitted)